Scanning Microscopy

Volume 1990
Number 4 *Fundamental Electron and Ion Beam Interactions with Solids for Microscopy, Microanalysis, and Microlithography*

Article 11

1990

Channelling and Related Effects in Electron Microscopy: The Current Status

Kannan M. Krishnan
National Center for Electron Microscopy, Berkeley

Scanning Microscopy Supplement 4, 1990 (Pages 157-170) 0892-953X/90$3.00+.00
Scanning Microscopy International, Chicago (AMF O'Hare), IL 60666 USA

CHANNELLING AND RELATED EFFECTS IN ELECTRON MICROSCOPY: THE CURRENT STATUS

Kannan M. Krishnan

National Center for Electron Microscopy
Materials and Chemicals Sciences Division
Lawrence Berkeley Laboratory
1 Cyclotron Road
Berkeley, CA 94720
Telephone Number (415) 540-6421

Abstract

The channelling or Borrmann effect in electron diffraction has been developed into a versatile, high spatial resolution, crystallographic technique with demonstrated applicability in solving a variety of materials problems. In general, either the characteristic x-ray emissions or the electron energy-loss intensities are monitored as a function of the orientation of the incident beam. The technique, as formulated in the planar geometry has found wide applications in specific site occupancy and valence measurements, determination of small atomic displacements and crystal polarity studies. For site occupancy studies, the appropriate orientations in most cases can be determined by inspection and the analysis carried out according to a simple classification of the crystal structure discussed in this paper. Concentration levels as low as 0.1 wt% can be easily detected. The reciprocity principle may be used to advantage in all these studies, if electron energy-loss spectra are monitored, as both the channelling of the incoming beam and the blocking of the outgoing beam are included in the formulation and analysis. The formulation in the axial geometry is an useful alternative, particularly for monatomic crystals. Localization effects are important if, either the experiment is performed in the axial geometry or if low atomic number elements ($z<11$) are detected. In general, the sensitivity to L-shells is lower compared to K-shell excitations. Other experimental parameters to be considered include temperature of the sample, the acceleration voltage and parallelism of the incident beam. Any detrimental effects of channelling on conventional microanalysis can be minimized either by tilting the crystal to an orientation where no lower order diffraction vectors are excited or by using a convergent probe such that a large range of incident beam orientations are averaged in the analysis.

Key Words: Channelling, Borrmann Effect, Site Occupancy, Localization, ALCHEMI, Crystal Polarity, Electron Energy-Loss Spectroscopy, Specific Site Valence, Cation Ordering, Dopants, Electron Microscopy, Inelastic Scattering

Introduction

The motion of charged particles in monocrystalline solids is strongly influenced by channelling and blocking effects. Even though these effects are well known in general and have been studied in great detail for some time (see [7] for an extensive review), there has been renewed interest in channelling and related phenomena, particularly in electron microscopy, over the past several years. In scanning electron microscopy, the primary emphasis has been on electron channelling patterns -- variation in the backscattered signal resulting from changes in the angle between the incident beam and the crystal lattice of the specimen -- with the ultimate goal of obtaining the crystallography and symmetry of a bulk sample as well as images of any defects that it may contain [16]. In transmission electron microscopy, most of the recent publications are related to the dependence of either the characteristic x-ray emissions or the characteristic energy-loss electron intensities on the orientation of the incident electron beam with respect to the sample [18,38]. A substantial portion of this work has had to do with the determination of the distribution [19] and valence [42] of impurity/alloying atoms in the various crystallographic sites (substitutional or interstitial) of a host lattice. Recent extensions of these ideas include the study of static atomic displacements [9], determination of the polarity of a crystal [43] and obtaining direct structure factor phase information [44].

The basis for all this work is the original observation of the anomalous transmission of x-rays in perfect crystals by Borrmann [1] and the subsequent comprehensive treatment of the dependence of characteristic x-ray production on electron beam orientation in monatomic single crystal films by Cherns, Howie and Jacobs [4]. However, much of the recent work on polyatomic crystals is directly due to the elegant realization [45] that the x-ray emissions from an atom of known distribution in the unit cell, can be used as a measure of the thickness averaged electron intensity on that specific crystallographic site. Then the ratio of this reference signal with respect to the intensities of the impurity/alloying elements can be interpreted directly in terms of the distribution of the latter in the crystallographic unit cell of the material [38].

In general for crystalline materials, an incident plane wave of electrons under conditions of strong dynamical diffraction sets up a standing wave within the crystal unit cell. The intensity modulations of this standing wave within the crystal

unit cell are primarily a function of the orientation of the incident wave with respect to the crystal. By suitable choice of orientations, the intensity maxima can be located at specific atomic or interstitial sites, or in the case of more complex polyatomic crystals, on different crystallographic sites in the unit cell. The coincidence of these intensity maxima on the atomic sites is normally accompanied by an enhancement of the characteristic ionization processes. Therefore signals associated with the ionization, such as x-ray emissions or the intensities of characteristic energy-loss electrons, also show a strong dependence on the spatial distribution of the standing wave in the unit cell. Using suitable spectrometers to monitor these ionization products, and taking ratios of the intensities of impurity/alloying elements with that of certain reference elements, a quantitative measure of the distribution of the former atoms among the various candidate sites can be derived [38]. The technique is only dependent on the degree of localization of the ionization event and the ability to select appropriate orientations that can separately resolve the candidate sites in that particular unit cell [18].

The original ratio formulation was applied to sites on specific crystallographic planes in the systematic or planar channelling orientation. In this geometry a single row of spots in the transmitted electron diffraction pattern is excited, such that the crystal potential is averaged in two orthogonal directions normal to the systematic row. In most simple cases, the appropriate systematic row can be determined by inspecting the crystal structure [18]. However, in complex crystals, it might be necessary to calculate the characteristic x-ray (or energy-loss) intensities as a function of orientation to determine the one that is appropriate [19]. A useful alternative to the above is electron channelling in the axial geometry [29,30]. An electron beam incident close to the zone axis excites many low-index Bragg diffraction vectors, thus setting up several simultaneous standing waves. For exact zone-axis orientations, this results in the electron beam being effectively channelled into columns and the current maximized on atomic strings. Further, the channelling effects are considerably enhanced in the axial case [28,32]. The details of analysis are essentially the same for both geometries, the only difference being that the latter investigates atomic columns instead of atomic planes. Additional differences between these two experimental arrangements will be elaborated in a later section.

There are some advantages if the intensity distribution of the inelastically scattered primary electron (electron energy-loss spectroscopy) is monitored instead of the characteristic x-ray emissions. The experimental arrangements are more flexible as both the incident and collection directions are selected independently, and both the channelling and blocking effects are incorporated in the analysis [46]. Thus intensities for different sites can be effectively squared by placing the detection aperture at an appropriate part of the diffraction pattern. Considerable enhancement of the inelastic scattering event can also be achieved by analyzing electrons scattered over large angles, i.e. larger transfer of momentum [26]. Finally, because of the superior energy resolution of EELS (~1eV), one can detect changes in oxidation states of the cations by measuring the small chemical shifts observed in the onset of the characteristic core-loss edges. Combining this chemical shift with the selective enhancement of the different

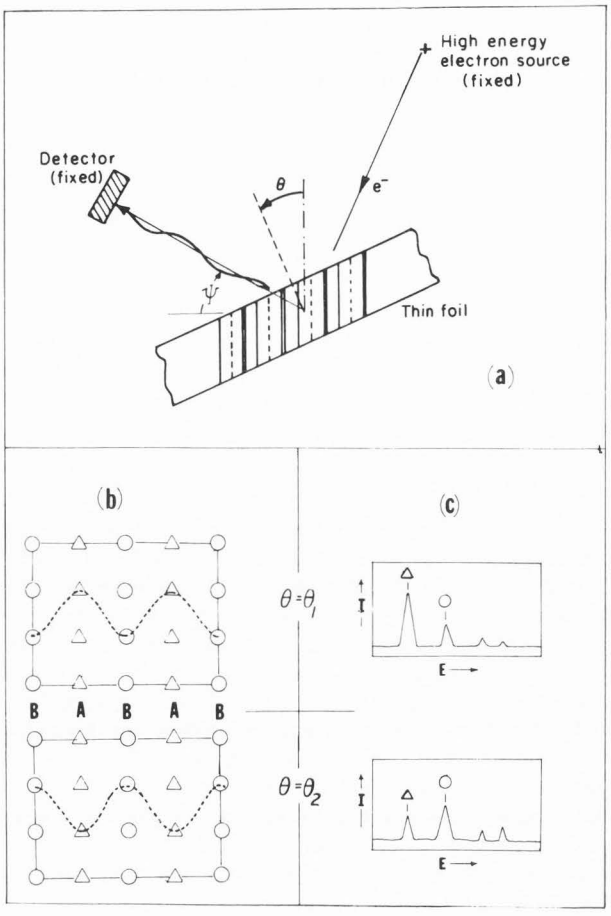

Figure 1. Physical principles of channeling enhanced microanalysis.

candidate sites by the appropriate choice of incident beam orientation, it is also possible to obtain specific site valence information [42].

Other manifestations of localized x-ray emissions have been observed and need further investigation in applied crystallography. A recent study addresses the measurement of small atomic displacements from the perfect lattice site in an imperfectly ordered alloy [9]. In addition to perfect localization, this method assumes that the perfect crystal wavefield is conserved in the distorted crystal. It is also possible to use such localized secondary emissions to obtain structure factor phase information associated with the lack of a centre of symmetry and to determine the polarity of a crystal [43,44]. This effect has been demonstrated directly by the observation of a large intensity difference for **g** and **-g** reflections along the polar direction in thin films of GaAs and InP.

These methods have been applied to a wide variety of crystallographic problems in magnetic materials [21,22], semiconductors [27,48], superconductors [37,47], intermetallic alloys [17], minerals [33,35] and ceramics [3]. The techniques are simple, involve no adjustable parameters and are relatively independent of the exact experimental conditions (particularly for the ratio method). Site occupancy

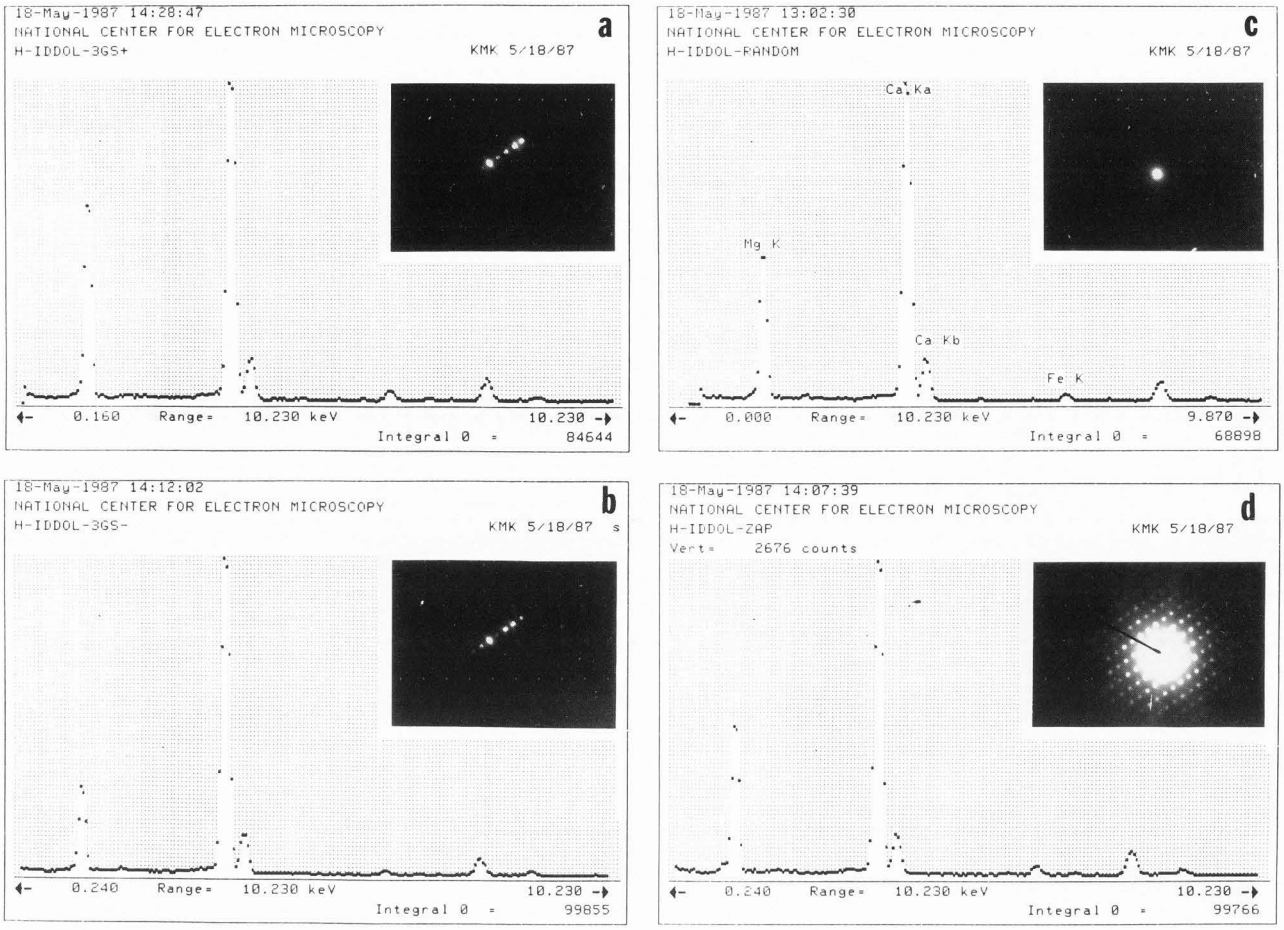

Figure 2 Dependence of x-ray emissions as a function of orientation for the dolomite structure. A [1000] systematic row is excited and localization on the Mg site is observed for a positive excitation error (s>0) of the third order Bragg diffraction (3g) condition (a). For 3g, s<0, the Ca site is selected (b). X-ray emissions for a zone axis (d) and a non-channelling orientation (c) are also shown for comparison.

measurements, using the ALCHEMI technique have been compared with other methods and the results are in good agreement [48].

This review will discuss the current status of these techniques, compare relative merits of the axial and planar channelling formulations, and EDXS vs. EELS detection. The formulation for different categories of crystal structures is summarized. Questions of localization, fundamental to the interpretation of such channelling data, are addressed. A relevant theoretical formulation is also presented. Other studies, currently being explored that are related to electron channelling, such as measurements of atomic displacements are introduced. Finally, some pertinent experimental details are considered. (For a more basic and tutorial discussion see either [18] or [39].)

Description of Techniques and Methods of Channelling

A simple arrangement for a channelling experiment, using characteristic x-ray emissions in a conventional transmission electron microscope (TEM), is shown in Figure 1a. The take-off angle (ψ) varies from 20^o to 70^o, based on the position of the EDXS detector, and is instrument dependent. However, for high take-off geometries, there is an additional freedom in the design of the experiment as the sample need not be tilted to any specific orientation to achieve optimal x-ray detection.

Under strong dynamical diffraction conditions, confirmed by the observation of Kikuchi lines, a standing wave pattern of the primary beam is set up in the crystal. A superposition of this standing wave on the projected crystal structure for the systematic or planar channelling orientation is shown in Figure 1b. In this condition, the wavefield in the crystal is two-dimensional (constant in a direction normal to the page) and its modulation on specific crystallographic planes is a function of the incident beam orientation. Secondary emissions, such as characteristic x-rays that are localized at atomic sites, are also a function of orientation (Figure 1c). If the Bloch waves peak on the A planes (orientation θ_1) an increase in the x-ray signal for the element occupying the site D is observed. For the other favourable orientation θ_2, the maximization is on the B planes and a corresponding increase for the elements occupying the site O would be noticed.

Figure 2 shows an example of the dependence of characteristic x-ray emissions on the orientation of the incident

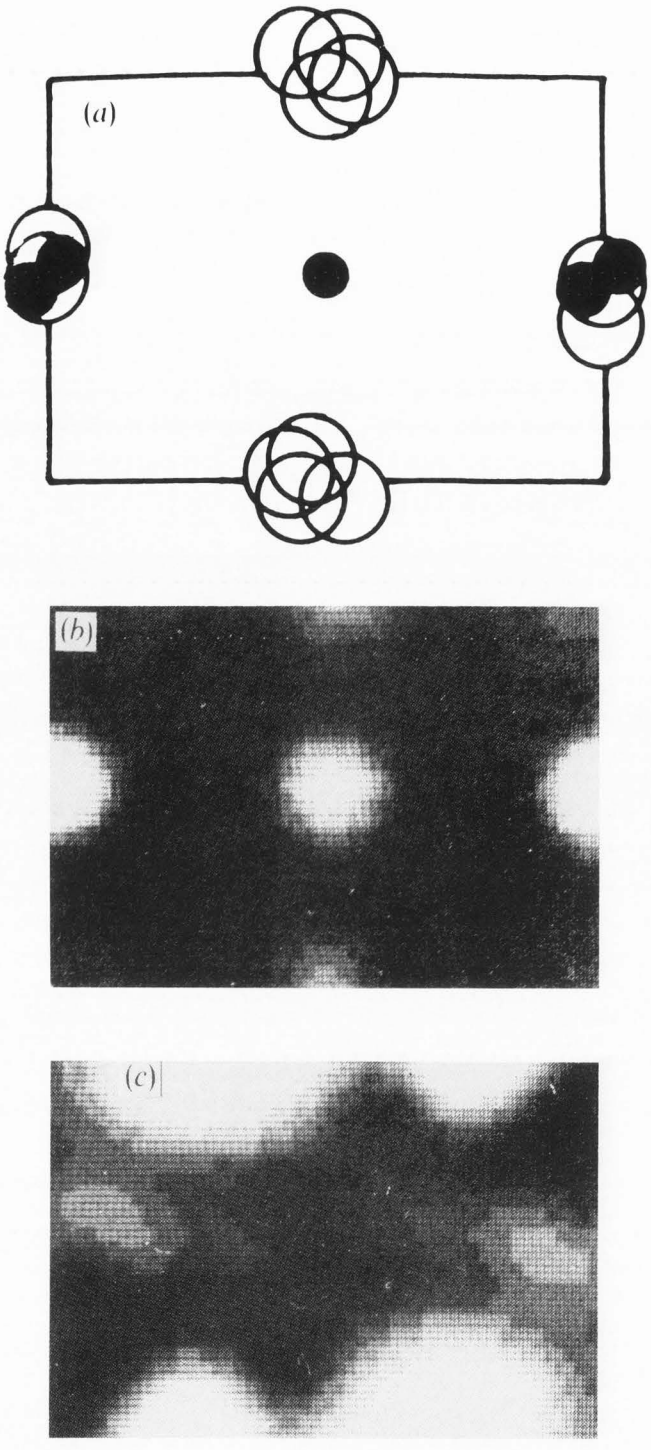

Figure 3 Projected structure of perovskite (a) in the <111> orientation. Titanium atoms are indicated by small filled circles, calcium by large filled circles and oxygen atoms by open circles. Calculated projection of the beam intensity in the <111> zone axis orientation for the perovskite structure showing peaking of the intensity on the projected atom sites (b). Tilting off the zone axis orientation results in the maxima being shifted to "open" channels (from [34]).

beam. For the dolomite structure (shown later), the best planar channelling conditions are when a [0001] systematic row is excited and the crystal is tilted such that the orientation corresponds to either small positive (s>0) or negative (s<0) excitation errors of the third order Bragg diffraction (3**g**) condition. In general, for s<0 the flux is concentrated on the heavier atoms (Ca) and for s>0, it is concentrated on the lighter atoms (Mg). In addition to a corresponding increase in x-ray intensities for these elements, a variation in the impurity Fe Kα intensity following that of Mg Kα is observed, suggesting similar site occupancy.

Electron channelling in the axial geometry is an useful alternative to the above [29,30]. An electron beam incident close to the zone axis excites many low-index Bragg diffraction vectors, thus setting up several simultaneous standing waves. For exact zone-axis orientations, this results in the electron beam being effectively channelled into columns and the current maximized on atomic strings. The calculated variation [34] of the electron beam intensity, for a perovskite structure projected in the <111> direction is shown in Figure 3. For the exact zone-axis orientation, the beam intensity peaks between the pairs of Ca atoms in the projected unit cell. For the off-axis orientation, there is a clear minimum occurring on the Ti sites and a shift toward open channels within the crystal structure. Again, variations in the intensity of x-rays of Ca and Ti (or impurities that either substitute for these elements or occupy interstitial sites) will be observed as a function of orientation.

The development of a meaningful technique of quantitative site occupancy determinations, utilizing the variations of x-ray intensities with orientation, is then largely dependent on both the ability to determine these favourable orientations and to obtain an independent measure of the electron intensity modulations over the unit cell. For electrons accelerated through kilovolt potentials the latter can be calculated using a dynamical many-beam theory [13]. However, the need for a theoretical prediction of the electron wave-field in the crystal can be avoided by using the x-ray emission from a reference atom of known distribution in the host crystal lattice. In the axial geometry, this reduces to finding a zone-axis orientation that separates the possible substitutional sites for the impurity onto different atomic columns in the beam direction, each with its own distinct reference atom. For a planar channelling geometry, the crystal potential is averaged in two orthogonal directions normal to the excited systematic row. In the simplest case, the crystal can be resolved in some projection into alternating layers of non-identical planes, each containing a distinct crystallographic site, and the appropriate orientation can be determined by inspection. For the dolomite structure (Figure 4a) the candidate sites occupy alternating planes at one-third the unit cell parameter along the c-axis. Hence by inspection, it can be concluded that a **g** = 0001 systematic row at the third order Bragg diffraction condition (Figure 2a, b) would give the best results.

If an *a priori* knowledge of the distribution of the relevant reference elements is available, their characteristic x-ray intensities could be used to obtain a measurement of the thickness-averaged electron wavefield intensity on specific atomic planes. In the case discussed above, the distribution of impurity or alloying element in the two possible sites is

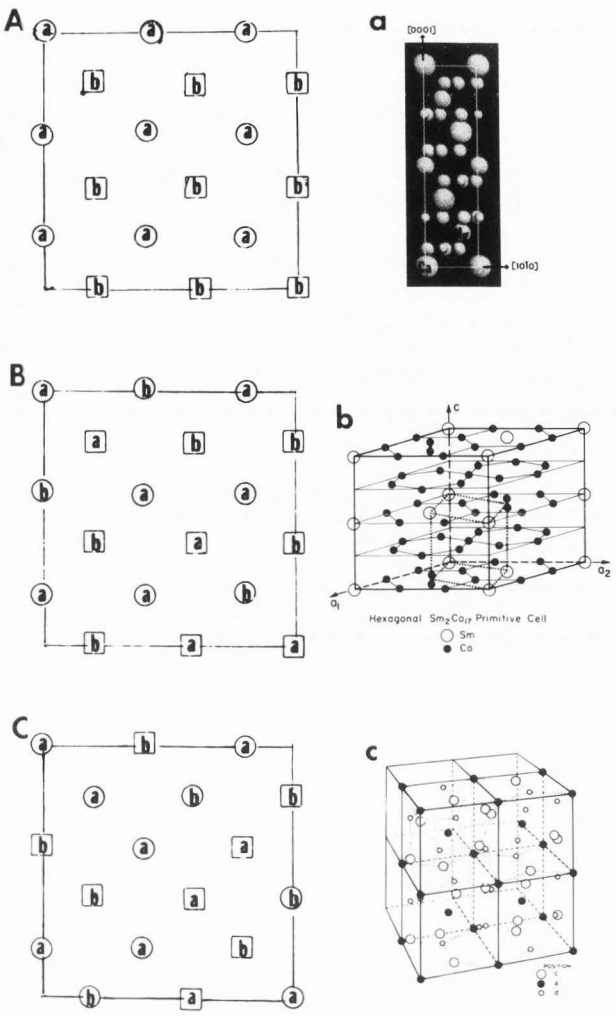

Figure 4 Classification of crystal structures for channelling enhanced microanalysis. Only two dimensional projections of relevance to the planar geometry are shown. (A) The simplest structure--the candidate sites can be projected on alternating planes each containing a specific reference atom. (a) an example: dolomite--alternating (0003) planes with Ca and Mg on the sites of interest. (B) same as (A) but without reference elements. (b) The Sm_2Co_{17} alloy where the sites of interest for the substitution of transition metal atoms are either on the Co planes or on the mixed Sm-Co planes, i.e. no internal reference. (C) The general structure--not easy to find simple projections with internal reference atoms. (c) The garnet structure bereft of the oxygen atoms.

determined by a method of ratios with respect to the intensities of the reference elements. Two different orientations, channelling ($3\mathbf{g}$, $s>0$ or $s<0$) and random (no lower order diffraction vectors excited) are used. For the dolomite structure, consisting of the two reference elements (Mg, Ca), the fraction of the impurity (Fe) substituting for Mg, C_{Fe} is then given by [10,38]

$$C_{Fe} = \frac{\frac{N^1_{Fe}}{N_{Fe}} - \frac{N^1_{Ca}}{N_{Ca}}}{\frac{N^1_{Mg}}{N_{Mg}} - \frac{N^1_{Ca}}{N_{Ca}}} \qquad (1)$$

where the Ns and N^1s are the observed intensities for these elements at the random and channelling orientations, respectively.

If the requirement of the existence of at least one species that lies exclusively on one of the alternating planes is violated (Figures 4b and 4B), but the candidate sites can still be projected onto alternating planes, more than one orientation along the systematic row will be required to perform the analysis. Further, in many practical alloys (Figure 4b), the alloying concentrations might be large enough to significantly alter the distributions of the constituent elements in the original compound. The precise number of orientations required will then be determined by the stoichiometry of the original compound and the actual distribution of the reference elements before alloying [20,22].

In the most general case (Figure 4C), a projection of the crystal structure that separates the candidate sites into planes, each with a specific site containing a specific internal reference element, cannot be found. For example, the garnet structure (Figure 4c) is such that the appropriate planar channelling orientations cannot be determined by inspection of the crystal structure or its projections [5], nor can the characteristic x-ray intensities be used as a measure of the thickness averaged electron intensity for any specific site. In such cases, the electron-induced characteristic x-ray emissions for different site occupations and different incident beam orientations have to be calculated and the experimental intensities refined using a constrained least-squares method to determine the occupancies.

Theory

The fast electron wavefunctions $\Psi(\mathbf{r})$ at any point r in the crystal can be written as a linear combination of Bloch waves [12,15]

$$\Psi(\mathbf{r}) = \sum_j \psi^j \sum_g C^j_g \exp[i(\mathbf{k}^j+\mathbf{g}).\mathbf{r}] \qquad (2)$$

where the amplitude ψ^j of the Bloch wave on branch j of the dispersion surface is $C_o{}^{j*}$. $C_g{}^j$ are the Bloch wave coefficients associated with the eigenvectors and the k^js are the eigenvalues. If anomalous absorption effects are included, the Bloch wave amplitudes attenuate with increasing depth. The coherent path of the Bloch wave is damped at depth z by the factor $\exp(-q^j z)$ and equation (2) is modified as

$$\Psi(\mathbf{r}) = \sum_j \psi^j \exp(-q^j z) \sum_g C^j_g \exp\{i(\mathbf{k}^j+\mathbf{g}).\mathbf{r}\} \; . \qquad (3)$$

The decrease in Bloch wave intensities results in an increase of the intensity of electrons diffusely scattered through the crystal. These diffusely scattered electrons behave as plane

waves [11] with uniform intensity at any depth given by

$$|\Psi_d(z)|^2 = 1 - \sum_j \psi^{j^2} \exp(-2q^j z) \quad . \qquad (4)$$

Representing the region of x-ray production as a δ-function broadened only by thermal vibrations at each atomic site, the imaginary part of the optical potential P(r), which describes the inner-shell ionization resulting in characteristic x-ray emissions [36], at any point **r** can be written as

$$P(\mathbf{r}) = \sum_g P_g \exp(i\mathbf{g}.\mathbf{r}) \quad . \qquad (5)$$

The Fourier components $P_g = P_o \exp(-\alpha g^2)$, where α is the normal Debye Waller factor and P_o is a constant. The x-ray production in the crystal is then given by [4]

$$X = \int |\Psi(\mathbf{r})|^2 P(\mathbf{r}) d^3\mathbf{r} + \int_o^t |\Psi_d(z)|^2 P_o dz \qquad (6)$$

where the first term is due to the coherent part and is integrated over the volume of the crystal. The second term is the incoherent contribution to x-ray production from the diffusely scattered plane waves. A detailed derivation of X using equation (6) is given elsewhere [4]. It suffices to say that the final expression contains three major contributions: an average intensity expected from non-crystalline materials, Bloch waves acting independently and Bloch wave interference terms.

However, if the anomalous absorption is neglected, the thickness integrated probability density of an electron at any coordinate **r** in the crystal is given by

$$\Psi\Psi^* = \sum_{jl} \psi^j \psi^{l*} \sum_{g,h} C_g^j C_h^{l*} \exp\{i(\mathbf{g}-\mathbf{h}).\mathbf{r} + \Delta\mathbf{k}_{jl}.\mathbf{r}\} \qquad (7)$$

where

$$\Delta k_{jl} = \mathbf{k}^j - \mathbf{k}^l \quad .$$

This approaches the result from an incoherent Bloch wave model asymptotically, with thickness:

$$\Psi\Psi^* = \Sigma |C_o^j|^2 \left| \sum_g C_g^j \exp(i\mathbf{g}.\mathbf{r}) \right|^2 \quad . \qquad (8)$$

This model fails for thin crystals but is exact for very thick crystals, provided that absorption is neglected. In the two-beam case, assuming the Bragg beam G to be at the exact Bragg position, equations (7) and (8) reduce to

$$I(x,z) = 1 - \sin(Gx)\sin(\Delta k\, z) \qquad (9)$$

and

$$\hat{I}(x,z) = 1 \qquad (10)$$

respectively. This is relevant to the interpretations of the orientation dependence of both x-ray emissions and characteristic energy-loss intensities, measured at orientations θ and -θ related by a mirror operation around the (111) planes of a non-centrosymmetric crystal [43,44]. It should be noted (see subsequent section) that the strong variations observed demand the inclusion of the Bloch wave interference terms in the theory.

Finally, the transition probability for a dynamical incident wave function scattering to a plane-wave final state through a δ-function scattering potential (neglecting thermal vibrations), integrated over a thickness t in the crystal, can be derived from equation (7). The rate of x-ray production is then

$$X_\delta = \int_o^t \Psi\Psi^* dz = \sum_{jl} \psi^j \psi^{l*} \sum_{g,h} C_g^j C_h^{l*} \exp\{i(\mathbf{g}-\mathbf{h}).\mathbf{r}\} \frac{\exp[\Delta k_{jl} t]-1}{i\Delta k_{jl}} \quad . \qquad (11)$$

Here $\psi^j = C_o^{j*}$ from the boundary conditions and the eigenvalues k^j are always real if absorption is neglected. Equation (11) can then be simplified as

$$X_\delta = \sum_{g,h} \exp[i(\mathbf{g}-\mathbf{h}).\mathbf{r}] \left\{ \sum_{j=l} C_o^{j*} C_g^{j*} C_o^l C_h^l + \sum_{j\neq l} C_o^{j*} C_g^{j*} C_o^l C_h^l \frac{\sin[(k^j-k^l)t]}{(k^j-k^l)t} \right\} \quad . \qquad (12)$$

where r is summed over all the relevant sites of interest in the unit cell.

Results of this theory for spinel and garnet structures are shown in Figures 5a,b. In the case of the garnet structure, which corresponds to the most general category (Figure 4C, in our classification), the characteristic x-ray emissions measured as a function of orientation were refined with respect to the calculated intensities, using a least squares procedure, to obtain probabilities of site occupations for rare-earth additions. Details are given elsewhere in the literature [19].

Choices in the design of channelling experiments

Axial vs. Planar Channelling.

There are a variety of choices to be exercised in the design of such electron channelling experiments. Foremost among them is the selection of the channelling geometry: planar or axial. In general, the axial geometry gives a stronger channelling effect [28, 32]. However, it is more difficult to find axial orientations which separate nonequivalent sites of the unit cell into distinct columns each containing a specific reference atom. On the other hand, finding planar orientations which separate candidate sites onto separate planes with specific reference elements is relatively straightforward for the majority of crystal structures. Hence the axial geometry is crystallographically more restrictive and the planar geometry is to be preferred for more complex structures. But for other structures, such as a monatomic matrix, the axial geometry is to be preferred. Such crystals containing a small quantity of impurities pose a particularly difficult problem in the planar

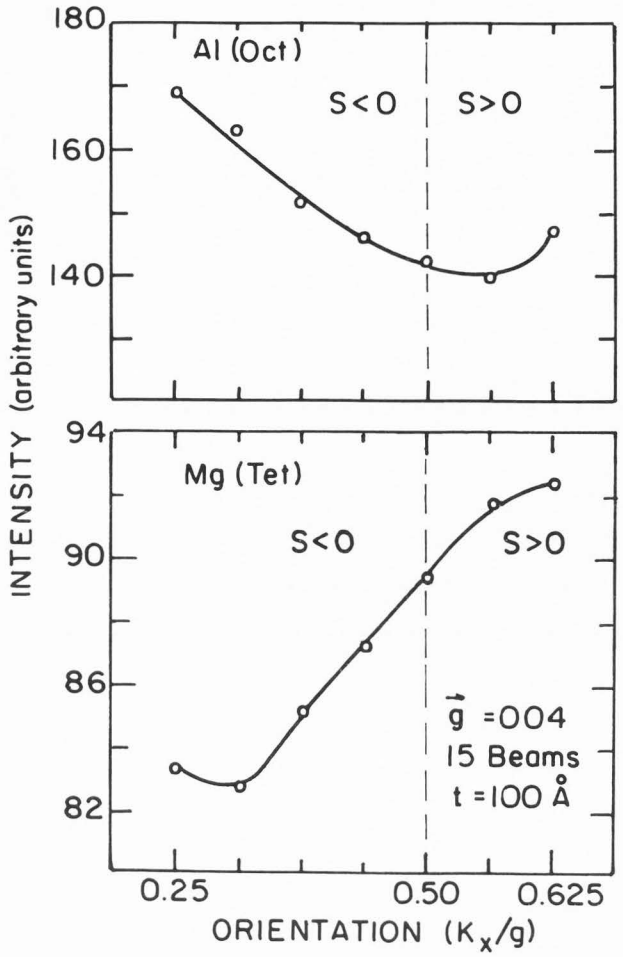

Figure 5a Calculated x-ray intensities using the δ-function localization theory for the spinel structure at various orientations along the [100] systematic row. Strong localization for the first order Bragg diffraction condition, i.e., (400), at s<0 for the Al site and at s>0 for the Mg site, are predicted by the theory and also observed experimentally.

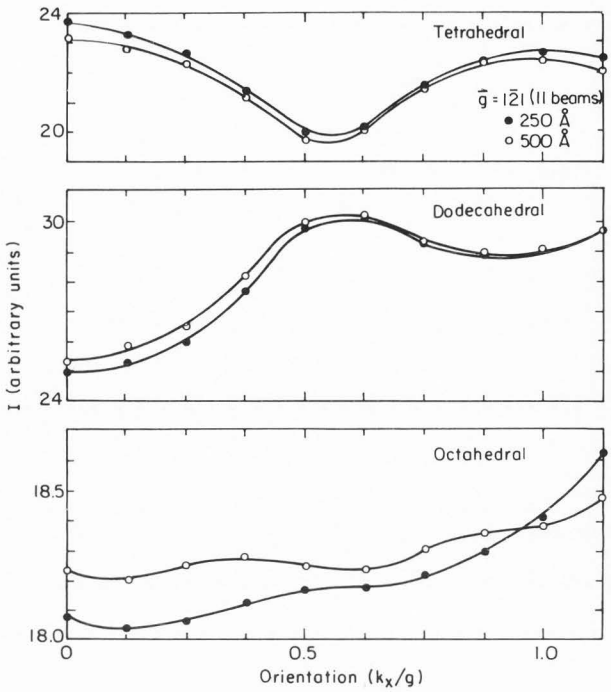

Figure 5b Calculations for the garnet structure. The g = 121 systematic row is found to be appropriate for performing channeling experiments.

geometry as independent reference signals for each of the potential sites are not available. Absolute x-ray yields from both the host and impurity species need to be measured, a task that demands very high instrument stability [49]. If the planar geometry is selected, each problem of site occupancy to be solved has to be tackled differently, beginning by classifying the crystal structure into one of the three categories discussed earlier (Figures 4 A,B,C) and proceeding with the appropriate formulation.

Attempts to use the axial geometry to obtain a quantitative analysis of site occupancies has met with mixed success [40]. It has been argued that these variations are due to the problems of delocalization of the inelastic scattering event, a phenomenon that is exaggerated in the axial geometry. However, methods for the correction of such delocalization effects in the axial geometry have been developed but they suffer from the limitations of being crystal structure and not atomic species dependent.

EDXS vs EELS.

Characteristic x-ray emissions and their corresponding energy-loss edges should show identical variation with the incident beam orientation. However, the principle of reciprocity can be applied approximately (although it is often a very good approximation) to the detection of the EELS signal. The sensitivity of EELS to site occupancy can thus be effectively squared by choosing the position of the detection aperture and placing it at an appropriate point in the diffraction pattern to be energy analyzed [46]. This is illustrated in Figures 6 and 7 at the **g** and **-g** orientations of a non-centrosymmetric crystal of GaAs [43]. Figures 6a,b show the variation of the energy dispersive x-ray spectra for the two orientations. The corresponding EELS data are shown in Figure 7. The incoming and the outgoing beams are indicated by the filled and open circles respectively. However, considerable enhancement of the sensitivity of EELS to the site occupancy can be achieved by a suitable choice of the direction of the outgoing beam, i.e. the diffraction of the exit wave or blocking is included (Figure 7c,d). This enhancement of site selectivity is similar to double alignment in particle channelling [31].

In addition, the localization of the inelastic scattering event can be enhanced by selecting only large angle scattering in EELS. It can be readily understood from a simple application of the uncertainty principle ($\Delta x * \Delta p \geq h$) that the distance ($\Delta x$) a fast electron can travel from the atom but still ionize it is inversely proportional to the momentum exchange (Δp) associated with the inelastic scattering event. For forward

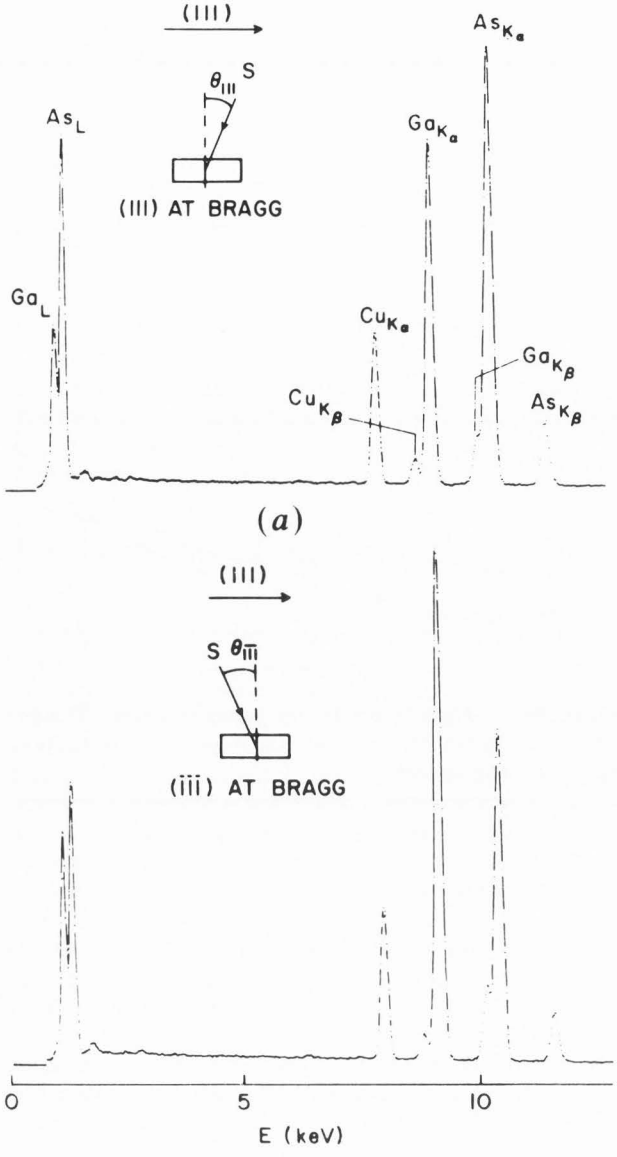

Figure 6 Orientation dependence of characteristic x-ray emissions for a GaAs sample (from [43]).

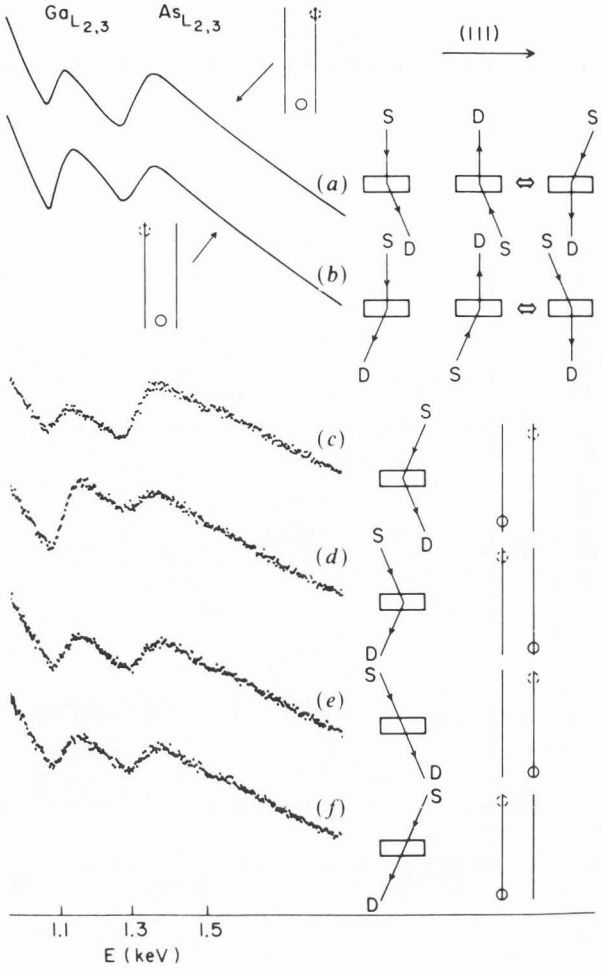

Figure 7 Electron energy loss spectra for the same two orientations shown in Figure 6. The position of the detector (dotted circle) can also be used to select the direction of the outgoing beam. Various sets of incident and outgoing beam geometries related by reciprocity arguments are also shown. Combining the channelling and blocking effects with enhanced localization, i.e., detecting electrons scattered through large angles only, gives the best results (c) and (d). Alternatively, the channelling and blocking effects can be made to cancel out the orientation dependence entirely--(e) and (f).

inelastic scattering it can be shown that

$$\Delta x_{max} = h/\Delta E \ (2 E_o/ m_e)^{1/2} \qquad (13)$$

where ΔE is the energy-loss, E_o is the primary energy and m_e is the mass of the electron. Using this simple expression, it can be shown that for a 100kV electron the maximum delocalization is such that it should not pose any problem for energy losses greater than 2keV [26]. However, by only analyzing electrons scattered over large angles, as indicated in Figure 7, the specific site sensitivity can be enhanced even for energy losses as small as 500eV. This is accomplished by shifting the detection aperture parallel to the Kikuchi band such that there is no change in the diffraction geometry.

The energy resolution of a commercial energy-loss spectrometer (~1eV using a conventional LaB_6 filament) is superior to that of EDXS detectors (~150eV for Mn Kα x-rays). This makes it possible to detect changes in the oxidation state of the cations by the small chemical shifts observed in EELS core edge features. In fact the 2eV chemical shift between Fe^{2+} and Fe^{3+} oxidation states can be routinely detected, particularly with the advent of the new parallel spectrometers. Combining this chemical shift with the selective enhancement of the different candidate sites, by the appropriate choice of incident beam orientations in a planar channelling experiment, it has been shown [42] that Fe^{3+} occupy octahedral sites while Fe^{2+} occupy tetrahedral sites in a

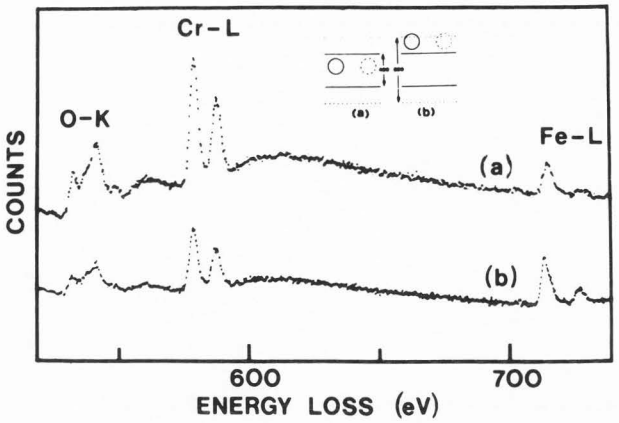

Figure 8A Electron energy loss spectra for a chromite spinel under two different incident beam orientations. For orientation (a) the localization is on the octahedral sites (Cr). For orientation (b) the tetrahedral sites (Fe) were enhanced [42].

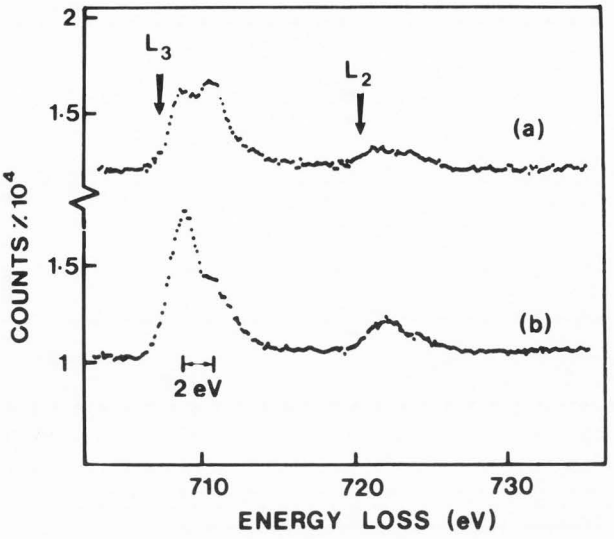

Figure 8B Details of the $FeL_{3,2}$ edge for the same orientations (a) and (b). The higher energy Fe^{3+} peak is enhanced for octahedral site localization [42].

naturally occurring chromite spinel. The relevant EEL spectra are shown in Figure 8a,b. For orientation (a) the octahedrally coordinated Cr^{2+} ions are selected. At the same orientation an increase in the intensity of the higher energy Fe^{3+} peak can also be observed. Note that in these experiments a significant enhancement in the localization is achieved by shifting the aperture parallel to the (400) Kikuchi lines such that only high angle scattered electrons are detected but without any change in the diffraction conditions.

In summary, even though EELS offers the possibility of obtaining more sophisticated information, in practice it is limited by problems of specimen thickness, multiple scattering and difficulties in the modelling of the background. On the other hand, EDXS is simple, straightforward and easy to interpret.

Measurement of atomic displacements.

Another potential application of such localization measurements in applied crystallography is the detection of small static displacements of the atoms from the perfect lattice sites. In addition to strong localization of the inelastic scattering event, the method recently developed [9] makes two important assumptions. The atomic displacements are assumed to be uncorrelated, i.e. the translational symmetry is preserved, and the wavefield in the distorted crystal is assumed to be the same as in the original undistorted one. However, for quantitative results the technique is complicated and requires a knowledge of the spatial modulation of the beam intensity in the crystal.

Qualitatively, these static atomic displacements can be measured using the simple ideas of planar channelling. As discussed earlier, in this formulation the beam intensity modulation in the crystal can be selected such that for negative excitation errors of the appropriate Bragg diffraction condition ($w<0$), it peaks on the atomic planes and for positive excitation errors it is maximized on the interstitial sites between the atomic planes. If the distribution of the two species of atoms A and B is such that on average A is closer to the lattice planes than B, the ratio of their x-ray intensities $\mathcal{R}(A/B)$ would be higher for $w<0$ when compared with that for $w>0$, provided that the inelastic events are strongly localized.

As of now, only semi-quantitative estimates of such displacements have been possible in a careful series of measurements on thin layers of $In_xGa_{1-x}As$. The displacements of the As atoms are of the order of 0.01nm [9]. It is expected that improvements of this technique can be made if more than two beams of the systematic row and the absorption of the Bloch waves are included in the theoretical estimates of the electron wavefield in the crystal.

Structure factor phase and crystal polarity measurements

The choice of an origin in a crystal unit cell determines the phase of a structure factor. Inelastic scattering events, such as characteristic x-ray emissions or electron energy-loss intensities, observed under the channelling conditions discussed in this paper contain direct information about the phase with which different elements contribute to a structure factor. The interference terms between the Bloch wave eigenstates contribute to these orientation dependent characteristic emissions [4]. It has been shown that by monitoring the localized emissions, information related to the structure factor phase associated with the absence of a center of symmetry can be obtained and the polarity of the crystal determined [44]. The variations in intensity of both the characteristic x-ray and energy-loss spectra , for incident beams forming angles θ and $-\theta$ relative to the polar plane [43] of GaAs are shown in Figures 6 and 7.

In the simple two beam theory including the interference terms discussed earlier, it has been shown that the intensity

distribution over the unit cell is given by

$$I(x,z) = 1 - \sin(G\,x)\,\sin(\Delta k\,z) \qquad (9)$$

where x is the distance from the reference planes (defined in the simplest case as those atomic planes parallel to the Bragg reflection planes with inversion symmetry) normal to the entrance surface, z is the distance from the entrance surface and Δk, which is proportional to the structure factor, is the difference between the wavevectors for the two Bloch waves [13]. For GaAs, the variation in intensity in the (111) direction (Figure 6) is in agreement with the above, i.e. equation (9).

If in such a standing wave experiment, the characteristic energy-loss intensities are monitored instead of x-rays, a four fold increase in the sensitivity to an absence of inversion symmetry is predicted based on reciprocity arguments. Indeed the reciprocity principle applies to the interference terms of the Bloch wave eigenstates and this is illustrated in Figure 7 where EEL spectra for GaAs at different diffraction geometries are shown. In EDXS the ratio As/Ga changes from 0.65 (111) to 1.5(111), whereas in EELS it can be improved to 0.45(111) and 2.20(111) respectively.

Effects of Localization on Channelling

Fundamental to the channelling phenomena discussed in this paper is the requirement that the inelastic scattering processes be strongly localized at the atomic sites. In this context a process is defined to be localized if its probability depends only on the (beam) current density at the close vicinity of the atomic nucleus.

Gjønnes and Høier [8] have estimated the spatial extent or 'radius' of the 1s orbitals to be approximately 0.002nm. Further, they suggested that any distribution, such as characteristic x-ray emissions, associated with the k-shell will also be spatially as narrow. Alternatively, an impact parameter <b>, defined as the expectation value of the distance at which the beam electron can transfer a specific quantity of energy to the core electron, can determine the degree of localization.

Estimating the time τ over which a virtual photon is exchanged between a fast electron and the excited particle and converting that, following Howie [14], using the uncertainty principle, to give an expression for the limiting value of the impact parameter, Bourdillon, Self and Stobbs derived a simple expression [2]:

$$\langle b \rangle = \frac{hv}{2\langle E \rangle} f \qquad (14)$$

where v is the velocity of the fast electron, <E> is the mean value of the energy-loss of the beam electron associated with the inelastic scattering event and f is a constant of order 1. It follows that for a prediction of the degree of localization for x-ray emissions, it is necessary to have a quantitative value for the mean energy <E> and/or mean momentum <q> transfer. On the other hand, in EELS experiments both q and E can be uniquely defined. For x-rays, the required mean values can be calculated [32]:

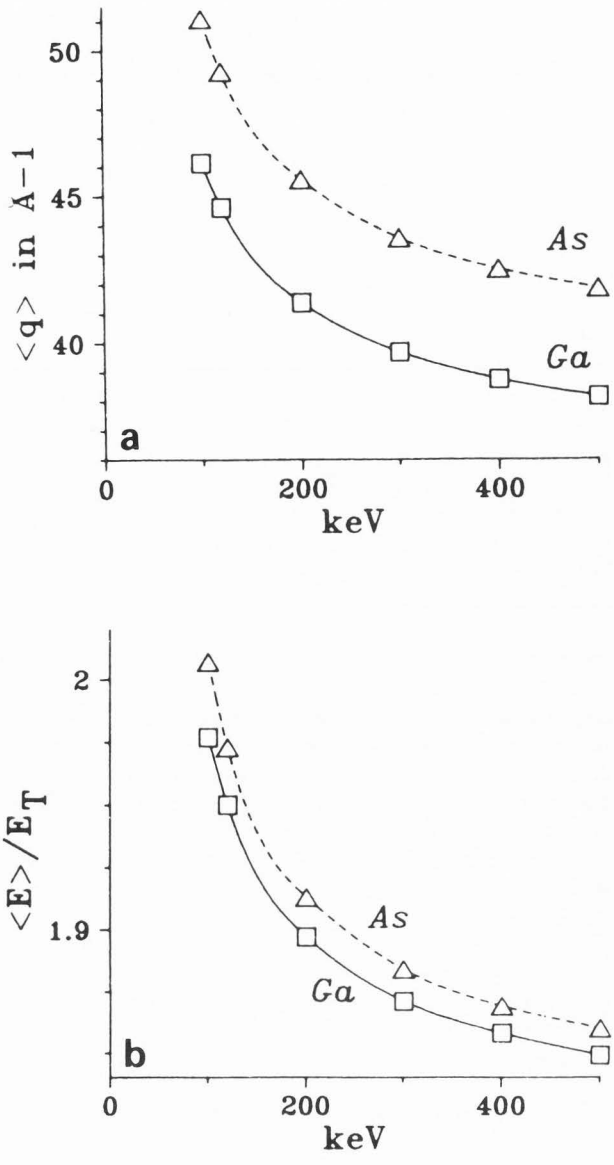

Figure 9 (a) Mean wave vector <q> transfer for Ga and As K-shell excitations as a function of incident beam energy. (b) Mean energy loss <E> ratio with respect to the ionization threshold energy E_T as a function of incident beam energy [32].

$$\langle E \text{ or } Q \rangle = \int_{E_T}^{E_{max}} \int_{q_{min}}^{q_{max}} (E \text{ or } q)\, \frac{d^2\sigma}{dE\,dq}\, dE\, dq\, \sigma_T \qquad (15)$$

where $d^2\sigma(q,E)/dq\,dE$ is the double differential energy-loss cross-section, σ_T is the total ionization cross-section and E_T is the threshold ionization energy. <q> and <E> calculated, using the above formula, are plotted in Figure 9a, b. Both show a monotonic decrease with the incident beam energy, Eo. <E> ~ 1.96 E_T at 120 kV and corroborate earlier estimates of 2.23E_T [2].

The impact parameter can also be calculated by a more

rigorous approach [32] where the degree of localization is considered to be dependent on both the change in the momentum of the primary electron and the change of state of the ejected core electron. In this (e,2e) scattering kinematics an "inelastic scattering potential" H(**r**) can be constructed for a hydrogenic scattering model, which can then be averaged, $H_{av}(\mathbf{r})$, over all angles of ejection. Using $[H_{av}(\mathbf{r})]^2$, which is closely related to the transition probability, an estimate of the mean square impact parameter, $\langle b_x \rangle$, can be calculated [32]. It suffices to say that this estimate is 35% smaller than that of Bourdillon, Self and Stobbs [2], i.e. $\langle b \rangle = 1.35 \langle b_x \rangle$.

For energy loss experiments, it can be shown from a simple application of the uncertainty principle that the distance a fast electron can pass from an atom and still ionize it is inversely proportional to the momentum exchange associated with the inelastic scattering event. Even though estimates of the impact parameter using (14) indicate that for losses less than 1keV the localization is inadequate, it has been experimentally demonstrated [26] that the specific site sensitivity for energy losses as small as 500eV (oxygen K-edge) can be detected by analyzing electrons scattered over large angles. This is accomplished in such a way (in planar channelling by shifting the detection aperture along the Kikuchi line perpendicular to the systematic row of interest) that only high-angle scattered electrons are detected without any change in diffraction geometry required for channelling.

From the above discussion it is obvious that there is a low energy limit below which localization effects are detrimental to performing such channelling experiments. Unfortunately, there is no agreement in the literature as to the exact energy value at which the thermal effects dominate the localization effects. Estimates range from a lower limit of 200eV [36] to 10keV [32]. However, it is generally agreed that as far as possible higher energy x-ray fluorescence should be used in channelling experiments to minimize localization effects, i.e. K-shell in preference to L-shell excitations, as the former involves greater energy and momentum transfer.

Comparing axial and planar orientations, it has been found that the latter has greater immunity to delocalization effects. When many beams are excited, as in the axial case, contributions from Fourier components with large **g**-vectors tend to localize the wavefield of the fast electron. In general, the number of excited reflections increase with the acceleration voltage, values of Fourier potentials or average atomic number of the specimen and axial orientation. Moreover, in the case of axial orientation it has been suggested [30] that experimental correction factors for localization can be determined with relative ease. There is no doubt that such measurements may be valid in particular cases where standards with uniform depth distribution of impurities can be prepared. However, one must be cautioned that the inelastic scattering potentials are fundamentally dependent on the crystal structure and hence these c-factors are not a function of the atomic species alone.

Finally, Spence et al. [40], have recently rederived the original ALCHEMI formulation to include localization effects. They have concluded that the original formulation remains the same if either d-function localization can be assumed or the thickness-averaged intensity in the neighbourhood of the atomic species of interest is a slowly varying function over the inelastic localization volume.

Experimental Considerations

These site-occupancy measurements can be routinely carried out on most commercial electron microscopes equipped with either an energy dispersive x-ray detector or an electron energy-loss spectrometer. The methods are, of course, subject to all the limitations of the two individual spectroscopic methods. Moreover, no special specimen preparation methods are required. However, since all intensities are thickness-averaged, the distribution of impurities in the crystal should be uniform with depth. Any bending or thickness changes under the probe are unimportant as both the impurity as well as the reference elements are affected the same way by any local change in orientation.

Performing these channelling experiments at low temperatures has some significant advantages [41]--the scattering potential is less attenuated in higher order g-vectors leading to a greater variation in the electron beam intensities on the different sites. In addition the amplitude of thermal vibration is considerably reduced. The latter is material-dependent and no improvement is expected if the mean free path for phonon excitation becomes appreciably larger than the specimen thickness.

These techniques give best results for a parallel collimated electron beam. However in most modern TEMs, the specimen is immersed in the magnetic field of the objective lens and the electron follows a helical path in the vicinity of the sample. It has been pointed out [5], that this configuration introduces both a radial and tangential component of parallelism. Further, it has been suggested [6] that the tangential component due to the helical trajectory is the dominant criterion of parallelism and that best results are obtained with a substantial probe convergence compared to a parallel beam, provided that the probe convergence is less than the operational Bragg angle. However, this effect is instrument-dependent and a simple experiment, taking into consideration all factors for optimal data collection, such as the convergence angle and primary lens excitation combinations, can be performed to obtain the best working conditions [23].

A systematic study of the combined effect of acceleration voltage and incident beam orientation on the orientation dependence of characteristic x-ray production in thin crystals has been carried out [24]. For the $MgAl_2O_4$ spinel compound, the orientation dependence undergoes a reversal in character above a particular voltage. This "inversion voltage", observed experimentally at ~270kV, is in agreement with earlier theoretical predictions [25]. This inversion behaviour is different from the critical voltage effect. In any case, the experiment should be performed at any fixed acceleration voltage for best results.

The ability to use convergent probes and yet observe these channelling effects (within the constraints discussed above) makes it possible to routinely achieve a spatial resolution of 10-40nm. However, the spatial resolution is also determined by the statistics of the EDX detection process. It is estimated that reasonable results can be obtained using a 20nm probe for a 10^{25} atoms/m^3 distribution of impurities. In order that the dynamical wavefunction be well-sampled in depth, the following simple criterion has to be satisfied [38]

$$\xi_g \, n \, A \geq 1 \qquad (16)$$

where ξ_g is the dynamical extinction distance for the reflection **g**, n is the uniformly distributed concentration and A is the projected area of the electron probe. Finally, the use of a higher brightness source, such as a field emission gun would, in principle, considerably improve the lateral spatial resolution of these techniques.

These channelling effects could play a detrimental role in conventional microanalysis. In most practical cases such errors can be eliminated either by tilting the crystal to a non-channelling orientation, i.e. no lower order diffraction vectors are excited, or by using a large illumination aperture such that the large convergence angle effectively averages over a wide range of incident beam orientations.

Acknowledgement

The author would like to acknowledge Dr. P. Rez for many helpful discussions. This work was supported by the Director, Office of Energy Research, Office of Basic Energy Sciences, Materials Science Division, U. S. Department of Energy under Contract No. DE-AC03-76SF00098.

References

1. Bormann G. (1941), Uber Extinktionsdiagramme von Quarz, Physik 42, 157-162.

2. Bourdillon AJ, Self PG, Stobbs, WM. (1981), Crystallographic orientation effects in energy dispersive x-ray analysis, Phil. Mag. A44, 1335-1350.

3. Chan HM, Harmer MP, Lal M, Smythe DM. (1984), Calcium site occupancy in $BaTiO_3$, Materials Research Society Symposium Proc. 31, 345-350.

4. Cherns D, Howie A, Jacobs MH. (1973), Characteristic x-ray production in thin crystals, Z. Naturforsch. 28A, 565-571.

5. Christenson KK, Eades JA. (1986), On parallel illumination conditions for ALCHEMI, Electron Microscopy Society of America Proc. 44, 622-623.

6. Christenson KK, Eades JA. (1986), On "parallel" illumination in the transmission electron microscope, Ultramicrosc. 19, 191-194.

7. Gemmell DS. (1974), Channelling and related effects in the motion of charged particles through crystals, Rev. Mod. Phys. 46, 129-227.

8. Gjønnes J, Høier R. (1971), Structure information from anomalous effects in diffuse scattering of electrons, Acta Cryst. A27, 166-174.

9. Glas F, Henoc P. (1987), Study of static atomic displacements by channelled-electron-beam-induced x-ray emission: Application to $In_{0.53}Ga_{0.47}As$ alloys, Phil. Mag. A56, 311-328.

10. Goo E. (1986), Reformulation of atom location by channeling enhanced microanalysis, Appl. Phys. Lett. 48, 1779-1779.

11. Hall CR. (1960), On the production of characteristic x-rays in thin metal crystals, Proc. Roy. Soc. A295, 140-163.

12. Heidenreich RD. (1962), Attenuation of fast electrons in crystals and anomalous transmission, J. Appl. Phys. 33, 2321-2333.

13. Hirsch PB, Howie A, Nicholson RB, Pashley D, Whelan MJ. (1965), Electron Microscopy of Thin Crystals (Butterworths, London).

14. Howie A. (1979), Image contrast and localized signal selection techniques, J. Microsc. 117, 11-23.

15. Humphreys CJ. (1979), The scattering of fast electrons by crystals, Rep. Progr. Phys. 42, 1825-1887.

16. Joy DC, Newbury DE, Davidson DL. (1982), Electron channeling patterns in the scanning electron microscope, J. Appl. Phys. 53, R81-R122.

17. Konitzer DG, Jones IP, Fraser HL. (1986), Site occupancy in solid solutions of Nb in the intermetallic compounds TiAl and Ti_3Al, Scripta Met. 20, 265-268.

18. Krishnan KM. (1988), Atomic site and species determinations using channeling and related effects in analytical electron microscopy, Ultramicrosc. 24, 125-142.

19. Krishnan KM, Rez P, Thomas G. (1985), Crystallographic site occupancy refinements in thin film oxides by channelling enhanced microanalysi, Acta Cryst. B41, 396-405.

20. Krishnan KM, Thomas G. (1982), Generalization of atom location by channelling enhanced microanalysis, J. Microsc. 136, 97-101.

21. Krishnan KM, Rez P, Mishra R, Thomas G. (1984), Determination of the specific site occupation of the rare earth additions in $Y_{1.7}Sm_{0.6}Lu_{0.7}Fe_5O_{12}$ thin films by the orientation dependence of characteristic x-ray emissions, Materials Research Society Symposium Proc. 31, 79-84.

22. Krishnan KM, Rabenberg L, Mishra RK, Thomas G. (1984), Site occupation of ternary elements in $Sm_2(CoTM)_{17}$ compounds, J. Appl. Phys. 55, 2058-2060.

23. Krishnan KM. (1987), When is parallel illumination best for ALCHEMI? Ultramicrosc. 23, 199-203.

24. Krishnan KM, Rez P, Thomas G, Yokota Y, Hashimoto H. (1986), The combined effect of acceleration voltage and incident beam orientation on the characteristic x-ray production in thin crystals, Phil. Mag. B53, 339-348.

25. Krishnan KM, Rez P, Thomas G. (1983), Effect of voltage on the orientation dependence of electron induced characteristic x-ray emissions, Proc. 7th Int. Conf. on HVEM, Berkeley, CA, 365-370. (reprint available from author)

26. Krivanek OL, Disko MM, Taftø J, Spence JCH. (1982), Electron energy loss spectroscopy as a probe of the local atomic environment, Ultramicrosc. 9, 249-254.

27. Liliental Z. (1983), On the point and line defects which are common to both degraded light emitting diodes and plastically deformed GaAs, J. Appl. Phys. 54, 2097-2102.

28. Otten MT, Buseck PR. (1987), The determination of site occupancies in garnet by planar and axial ALCHEMI, Ultramicrosc. 23, 151-158.

29. Pennycook SJ, Narayan N. (1985), Atom location by axial-electron-channeling analysis, Phys. Rev. Lett. 54, 1543-1546.

30. Pennycook SJ. (1988), Impurity lattice and sublattice location by electron channeling, Scanning Microsc. 2, 21-32.

31. Picraux ST, Brown WL, Gibson WM. (1972), Lattice location by channeling angular distribution: Bi implanted in Si, Phys. Rev. B6, 1382-1394.

32. Rossouw CJ, Maslen VW. (1987), Localization and ALCHEMI for zone axis orientations, Ultramicrosc. 21, 277-290.

33. Rossouw CJ, Turner PS, White TJ. (1988), Axial electron-channeling analysis of perovskite II. Site identification of Sr, Zr and Cl impurities, Phil. Mag. B57, 227-241.

34. Rossouw CJ, Turner PS, White TJ. (1988), Axial electron-channeling analysis of perovskite. I. Theory and experiment for $CaTiO_3$, Phil. Mag. B57, 209-225.

35. Self PG, Buseck PR. (1983), High resolution structure determination by ALCHEMI, Electron Microscopy Society of America Proc. 41, 178-181.

36. Self PG, Buseck PR. (1983), Low-energy limit to channeling effects in the inelastic scattering of fast electrons, Phil. Mag. A48, L21-L26.

37. Shindo D, Hiraga K, Hirobayashi H, Tokiwa A, Kikuchi M, Syono Y, Nakatsu O, Kobayashi N, Muto Y, Aoyagi E. (1987), Effect of Co substitution on T_c in $YBa_2Cu_3O_7$, Japan. J. Appl. Phys. Lett. 26, 1667-1669.

38. Spence JCH, Taftø J. (1983), ALCHEMI: a new technique for locating atoms in small crystals, J. Microsc. 130, 147-154.

39. Spence JCH, Taftø J. (1982), Atomic site and species determination using the channelling effect in electron diffraction, Scanning Electron Microsc.; 1982:II, 523-531.

40. Spence JCH, Kuwabara M, Kim Y. (1988), Localization effects on quantification in axial and parallel ALCHEMI, Ultramicrosc. 26, 103-112.

41. Spence JCH, Graham RJ, Shindo D. (1985), Cold ALCHEMI: Impurity atom site location and the temperature dependence of dechannelling, Materials Research Society Symposium Proc. 62, 153-162.

42. Taftø J, Krivanek OL. (1982), Site specific valence determinations by electron energy loss spectroscopy, Phys. Rev. Lett. 48, 560-563.

43. Taftø J. (1987), Reciprocity in electron energy-loss spectra from non-centrosymmetric crystals, Acta Cryst. A43, 208-211.

44. Taftø J. (1983), Structure-factor phase information from two-beam electron diffraction, Phys. Rev. Lett. 51, 654-657.

45. Taftø J. (1982), The cation distribution in a (Cr, Fe,Al, Mg)$_3O_4$ spinel as revealed from the channelling effect in electron induced x-ray emission, J. Appl. Cryst. 15, 378-385.

46. Taftø J, Krivanek OL. (1982), Characteristic energy losses from channeled 100keV electrons, Nuc. Inst. and Methods 194, 153-158.

47. Taftø J, Sabatini RA, Suenaga M. (1985), Crystal site occupancy of alloying elements in polycrystalline Nb_3Sn superconductors by electron channeling, Electron Microscopy Society of America Proc. 43, 196-199.

48. Taftø J, Buseck PR. (1983), Quantitative study of Al-Si ordering in an orthoclase feldspar using an analytical transmission electron microscope, Amer. Mineral. 68, 944–950.

49. Taftø J, Spence JCH, Fejes P. (1983), Crystal site location of dopants in semiconductors using a 100keV electron probe, J. Appl. Phys. 54, 5014-5015.

Discussion with Reviewers

J. C. H. Spence: The two beam dynamical theory depends only on $|u_g|^2$ and is therefore independent of the phase of all structure factors. How is it possible therefore to analyse the data for figures 6 and 7 for acentric GaAs using equation 9?
Author: Traditionally, the total intensity of the wavefield has been expressed as a sum of the individual Bloch wave intensities. This results in a thickness independent intensity modulation. Further this intensity modulation is identical near the Bragg position for G and -G reflections. However, if the interference terms between the Bloch waves are included, the well-known thickness oscillations and an asymmetry around the reference planes result. In particular, instead of a uniform intensity over the unit cell at the exact Bragg position, we now have equation 9 where x is the distance from the reference plane.

S. J. Pennycook: One of the strengths of the Bloch wave treatment of dynamical diffraction is that absorption can be handled quite easily, even in non-centrosymmetric crystals. Channelling experiments are always designed to maximize the change in the excitation of some localized interaction with incident beam orientation. Since absorption is localized there will always be a strong change in absorption with orientation. In the simple ratio methods, this factor is removed, but if one is trying to match quantitatively the experiemental and calculated rocking curves for impurities on different sites, then it would seem essential to include absorption as accurately as possible. How sensitive are measurements of site occupancies or small atomic displacements to the treatment of absorption, and does the current understanding of absorption in fact represent the practical limit to the quantitative interpretation of channeling experiments?.
Author: For a quantitative matching of experimental and calculated rocking curves, it is important to include absorption as accurately as possible. However, there are very few examples in the literature where absorption has been taken into consideration. Glas and Henoc [9] conclude that the main effects of absorption are to diminish the amplitude of the variation with incidence angle and to dampen subsidiary oscillations. It has also been argued that the strength of the channelling effects [40] is limited by absorption effects for low order reflections ($g<b$) but by localization for higher order reflections. Here $1/b$ is defined as the width of the localization function in real space. From the practical point of view, an improved understanding of absorption and localization will considerably enhance our ability to quantitatively interpret channelling data.

S. J. Pennycook: The problem of delocalization of the inner shell excitation is particularly severe for semiconductors and metal alloys which tend to have relatively small spacings between atomic strings. Pennycook [30] has shown how delocalization effects can be included quantitatively by reformulating the analysis in terms of the normalized channeling effect for each element rather than simply the ratio of counts. Equation (1) would be written as follows:

$$C_{Fe} = \frac{\frac{1}{c_{Fe}}\left[\frac{N^1_{Fe}}{N_{Fe}} - 1\right] - F\frac{1}{c_{Ca}}\left[\frac{N^1_{Ca}}{N_{Ca}} - 1\right]}{\frac{1}{c_{Mg}}\left[\frac{N^1_{Mg}}{N_{Mg}} - 1\right] - \frac{1}{c_{Ca}}\left[\frac{N^1_{Ca}}{N_{Ca}} - 1\right]}$$

where the c factors account for the reflection of the measured channeling effect due to delocalization effects. This formulation also allows for situations where the total substitutional fraction F_S is not unity. For perfect localization the c factors are all unity and for F_S=1 your Equation (1) is recovered.

By referring the c factors to the normalized channelling effects in this way, they are found to be remarkably insensitive to the actual channeling effect measured experimentally (S. J. Pennycook, *Ultramicroscopy* **26**, 239, 1988). They can be calculated quite accurately from a simple classical model of the inelastic scattering process and in fact, to a good approximation, are simply the ratio of the electron flux at a distance of the average impact parameter from the atomic string to the peak flux on the string. Since they are ratios, they need only be calculated (or measured) once for a particular channelling geometry.

The electron flux calculation can be performed either by Bloch wave methods or using the multislice routines popular for simulating high resolution images. Of course, the correction depends on crystal structure, but one calculation of the flux distribution gives the c factors for all elements. With this approach it is not necessary to predict the actual channeling effect obtained experimentally which would be exceedingly difficult, perhaps impossible, and would require a calculation for each experiment. Hence, the essential simplicity of the ratio method is retained, but the methods are extended to situations which cannot otherwise be handled. Could the author comment on this approach?

Author: This approach seems interesting but there are some important points to be addressed. First, the "average impact parameter" is element specific. Hence the electron flux has to be calculated at different distances for different atomic strings. This is complicated by the fact that there is still considerable debate on the exact nature of the localization parameters. Second, the electron flux is crystal structure specific. Hence, even though this approach retains the essential simplicity of the ratio method, it will involve detailed computations for each experimental arrangement.

P. Schattschneider: In ALCHEMI, it can be said that an x-ray emerges from a particular (equivalent) site in the lattice. Is it meaningful to ask from which single atom or ion a given x-ray photon comes?

Author: No, there is no situation that I am aware of where it would be relevant to ask this question. Further, the measurements are always carried out under strong dynamical scattering and the intensities are thickness integrated. Under these conditions, it is only meaningful to address occupation of equivalent sites.

D. Newbury: Although energy dispersive x-ray spectra from thin foils are inherently simpler than electron energy loss spectra, there is the possible problem of interferences which are the result of the coherent Bremsstrahlung process. In your experiments, do coherent Bremsstrahlung peaks cause any degradation in the practical detection limits which you can achieve with the channeling technique?

Author: No, these measurements are generally not degraded by coherent Bremsstrahlung peaks.